

## **Proof of concept demonstration of CONFIDANTE (CONFirmation using a Fast-neutron Imaging Detector with Anti-image Null-positive Time Encoding)**

P. Marleau\*<sup>1</sup>, R. Krentz-Wee<sup>2</sup>, and P. Schuster<sup>3</sup>

<sup>1</sup>*Sandia National Laboratories, Livermore, CA 94551*

<sup>2</sup>*University of California Berkeley, Department of Nuclear Engineering*

<sup>3</sup>*University of Michigan, Department of Nuclear Engineering*

\*pmarlea@sandia.gov

### **Abstract**

Future nuclear arms reduction treaties may require technical means to provide confidence that items being dismantled and/or removed from a regime are nuclear warheads as declared. Because the radiation signatures of nuclear warheads carry information sensitive to key attributes unique to their nature, radiation detection measurements are often looked to as a means of providing this confidence. However, for the same reason, data collected while confirming certain attributes might reveal sensitive design information that treaty parties will likely wish to protect. Overcoming the hurdle of verifiably using unique radiation signatures to provide confidence that an item is as declared, while simultaneously protecting sensitive design data, has been the focus of several decades of research and development. Generally, an information barrier (IB) is conceived to segregate this data from the view of monitoring parties. However, a balance must be struck between a monitoring party's ability to authenticate a measurement process and the segregation of any sensitive data collected and its subsequent analysis. Ideally, a comparison measurement and the data collected could be monitored in real time to provide confidence in its authenticity. We will present the results of proof of concept demonstrations of CONFIRMATION using a Fast-neutron Imaging Detector with Anti-image Null-positive Time Encoding (CONFIDANTE), a time-encoded imaging system (TEI) that may enable this capability. A TEI with a mask designed such that the pattern on one half of the cylinder is accompanied by its anti-pattern on the opposing side of the cylinder will exhibit an unmodulated detection rate if and only if two objects placed on opposite sides of the system are identical in geometry and activity. Because a positive confirmation is indicated by a constant rate at all times, a monitoring party might be allowed full access to the instrument before, during, and after confirmation without risk of leaking sensitive information.

## Introduction

Over the last several decades, considerable effort has been committed to the development of measurement systems that are capable of verifying that an item declared to be a warhead is as declared. These warhead confirmation systems must strike a balance between the desires of the warhead owner, or host, who wants to protect sensitive information, and the monitoring party, who may wish to use that sensitive information to verify the inspected item is a warhead. Systems have been developed that accomplish this by measuring sensitive information that is used to confirm a treaty accountable item (TAI) while sequestering that sensitive information behind an information barrier (1). These meet the needs of the host but places the onus on the monitor to authenticate the hardware, firmware, and software.

The warhead confirmation method presented in this work does not load sensitive information into the system at any time, and could therefore allow an inspecting party to not only view the data after a measurement, but also potentially access the associated equipment and data during the measurement. By using time-encoded imaging (TEI), a method in which the time modulation of radiation emitted from an object is used to construct an image (2), the projection of one object is added to the complement of the projection of another object at all times as illustrated in Figure 1. If the two objects are identical, the system measures only statistical noise. If the objects differ in shape or activity, then the count rate will exhibit excess variance around the mean value as the mask modulates their signals. Therefore, one way of measuring how alike two objects are is to measure how closely the distribution of detected count rates as a function of mask rotation angle follows a Poisson-distributed variable (3).

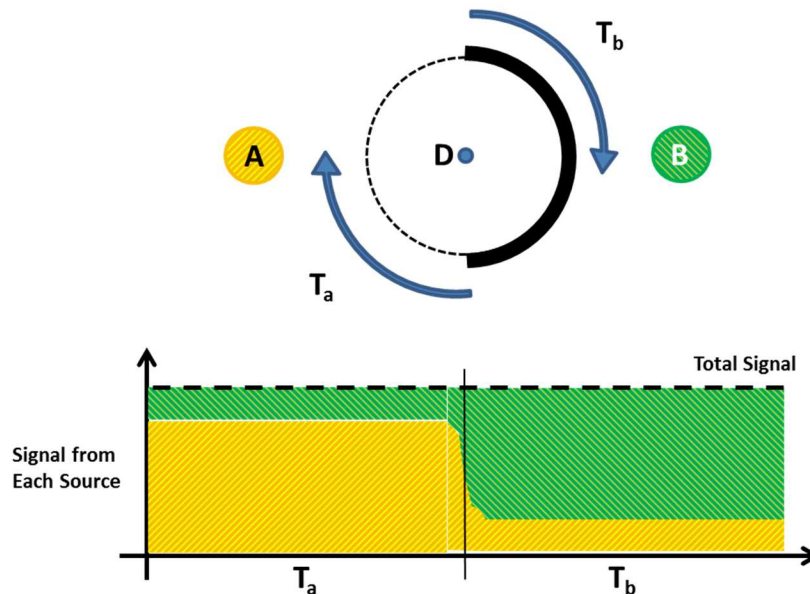


**Figure 1 – An example of the simplest anti-symmetric mask, a half-cylinder. The top shows two objects, A and B, on opposite sides of detector D, with the mask rotating around the detector. The bottom shows the count rate in the detector as a function of time as the mask rotates and the contribution to the total count rate from each object changes.**

If successful, the only recorded information will be a constant count rate within counting statistics, indicating a positive comparison. Therefore, a monitoring party might be allowed full access to the instrument before, during, and after the confirmation measurement without risk to sensitive information. The TEI system demonstrated in this work, dubbed CONFIDANTE (CONFirmation using a Fast-neutron Imaging Detector with Anti-image Null-positive Time Encoding) was specifically adapted for warhead verification by designing a mask with anti-symmetry such that the pattern on one half of the cylindrical mask is the inverse of the other half. Consisting of only a single radiation detector and a rotating mask to modulate the radiation field, CONFIDANTE is also simple, facilitating equipment authentication.

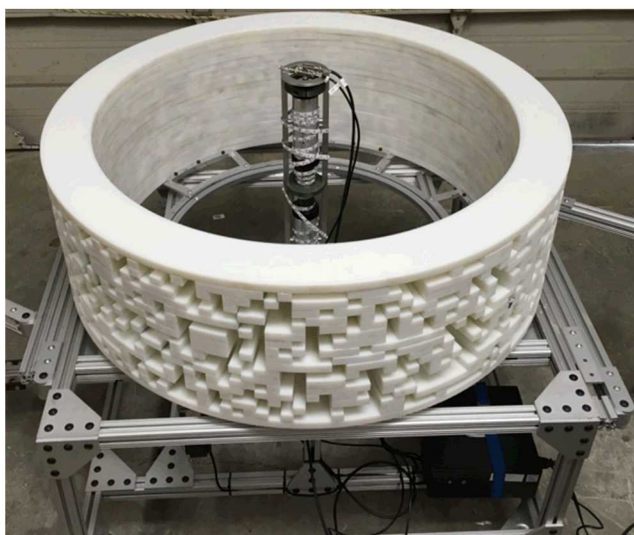


**Figure 2 – Photograph of the of the CONFIDANTE system.**

### **The Prototype CONFIDANTE System**

A two-dimensional TEI mask having the required anti-symmetric properties was designed and constructed. The mask, shown in Figure 2, comprises a stack of nineteen 1.9 cm thick sheets of High Density Polyethylene (HDPE) cut into a cylindrical mask/aperture pattern by water jet from a single piece. Each mask element is a wedge with angular width of 2.4 degrees, inner radius of 44.92 cm and outer radius of 55.08 cm. The randomly generated aperture pattern with the best imaging performance on a simulated test source distribution out of 100 randomly generated patterns was selected.

Along the axis of the cylindrical mask are two 2.54 cm diameter, 2.54 cm deep cylindrical stilbene organic scintillator detector pixels coupled to 5.08 cm Hamamatsu model 6094 photomultiplier tubes (PMTs). The centers of the detector pixels are positioned 5.08 cm above and below the centerline of the mask.

The current signals from the PMTs are digitized by a CAEN DT5720 250 MHz, 14-bit digitizer and read out via USB by a laptop PC. The encoder position is also read by USB in a separate thread. The digitizer and computer clocks are synchronized at the beginning of each measurement and are used to assign a mask angular orientation to every recorded event. Pulse shape discrimination (PSD) allows the gamma-ray and fast neutron counts to be separated in offline analysis as a function of rotation angle.

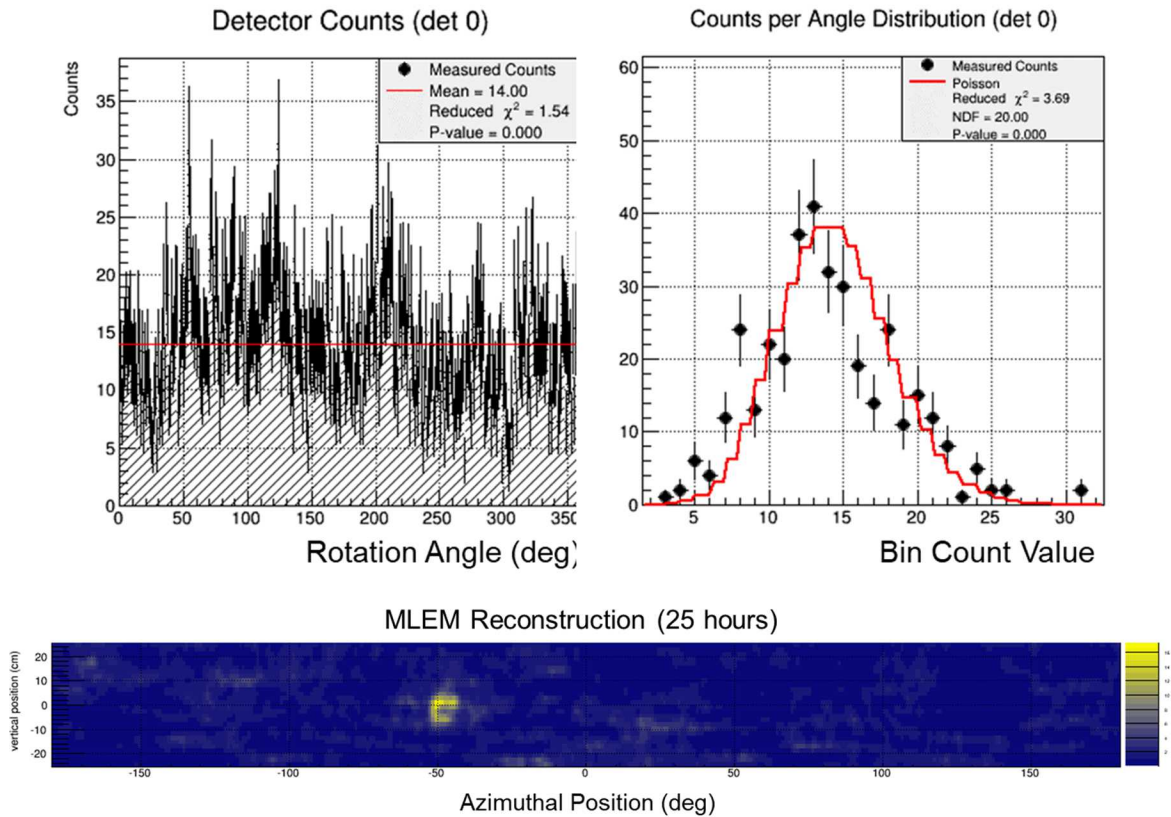


**Figure 3 – The number of fast neutron counts versus mask rotation angle (top left) and distribution of count values per degree (top right) from one detector for a two-hour measurement of the spherical PuO<sub>2</sub> shell and the MLEM reconstructed image from a 25 hour measurement (bottom).**

To demonstrate that the CONFIDANTE prototype is a functional two-dimensional TEI, the system was taken to Lawrence Livermore National Laboratory (LLNL) to measure their plutonium dioxide (PuO<sub>2</sub>) hemispherical shells. Two hemispherical shells were fit together to form a single spherical shell and placed at an angular orientation of -50 degrees with a center to mask edge distance of 40 cm. Figure 3 presents the number of counts versus mask rotation angle and distribution of count values in each 1-degree bin for two hours of data. A mean fast neutron count rate of 0.7 neutrons/second provides a mean count value of 14.0 per degree of mask rotation for this dwell time. It can be seen that the variance of this distribution is significantly different than what would be expected from a constant rate as indicated by a reduced  $\chi^2$  value

against the Null hypothesis (that the rate is constant with rotation angle) of 1.54, giving a p-value less than 0.001.

Further, the fast neutron count distribution as a function of mask rotation angle is used to reconstruct a two-dimensional image using a Maximum Likelihood Expectation Maximization (MLEM) algorithm (4). The hollow sphere distribution can be seen at the expected angular orientation and height.

### Proof-of-Concept Results

Two experiments are presented to demonstrate positive and negative results from measurements of distributed sources, i.e., one experiment with two identical objects and one with two different objects. These measurements were performed with LLNL's PuO<sub>2</sub> hemispherical shells. Each hemisphere was coupled to a solid HDPE hemisphere of the same diameter as the PuO<sub>2</sub> hemispheres. In the first experiment, the spheres were arranged with the PuO<sub>2</sub> hemispheres positioned on opposite sides of the mask, as shown in Figure 4. They were aligned such that the center of the sphere was 40 cm from the edge of the mask and vertically aligned with the center row of the mask. Alignment was checked using a laser pointer oriented outward from an opening in the center row of the mask. This represents a true positive test case in which the two objects should be identical.



**Figure 4 - CONFIDANTE with two LLNL PuO<sub>2</sub> hemispheres facing the central detector. Each hemisphere was coupled to a solid HDPE hemisphere on their backsides.**

. Figure 5 presents the number of counts versus mask rotation angle and distribution of count values in each 1-degree bin. It was found that 25 hours of data was required for statistical convergence as determined by tracking the Null hypothesis  $\chi^2$  as a function of time. A mean fast neutron count rate of 0.8 neutrons/second provides a mean count value of 15.9 per degree of mask rotation for this dwell time. To test whether the variance of this count distribution is

consistent with the expectation of a constant rate, we calculate the reduced  $\chi^2$  against the Null hypothesis (that the rate is constant with rotation angle). Reduced  $\chi^2$  values of 1.07 against the counts vs. rotation angle (Figure 5, top left) and 0.93 against the distribution of count values per degree (Figure 5, top right) are obtained. This corresponds to p-values of 0.172 and 0.55 respectively, indicating that the Null hypothesis cannot be rejected. Therefore, this measurement *is* statistically consistent with a constant rate indicating confirmation that these two items are identical.

Further, the fast neutron count distribution as a function of mask rotation angle can be used to reconstruct a two-dimensional image MLEM. The resulting image shown in Figure 5, bottom, does not reveal any imaging information and is consistent with noise as expected.

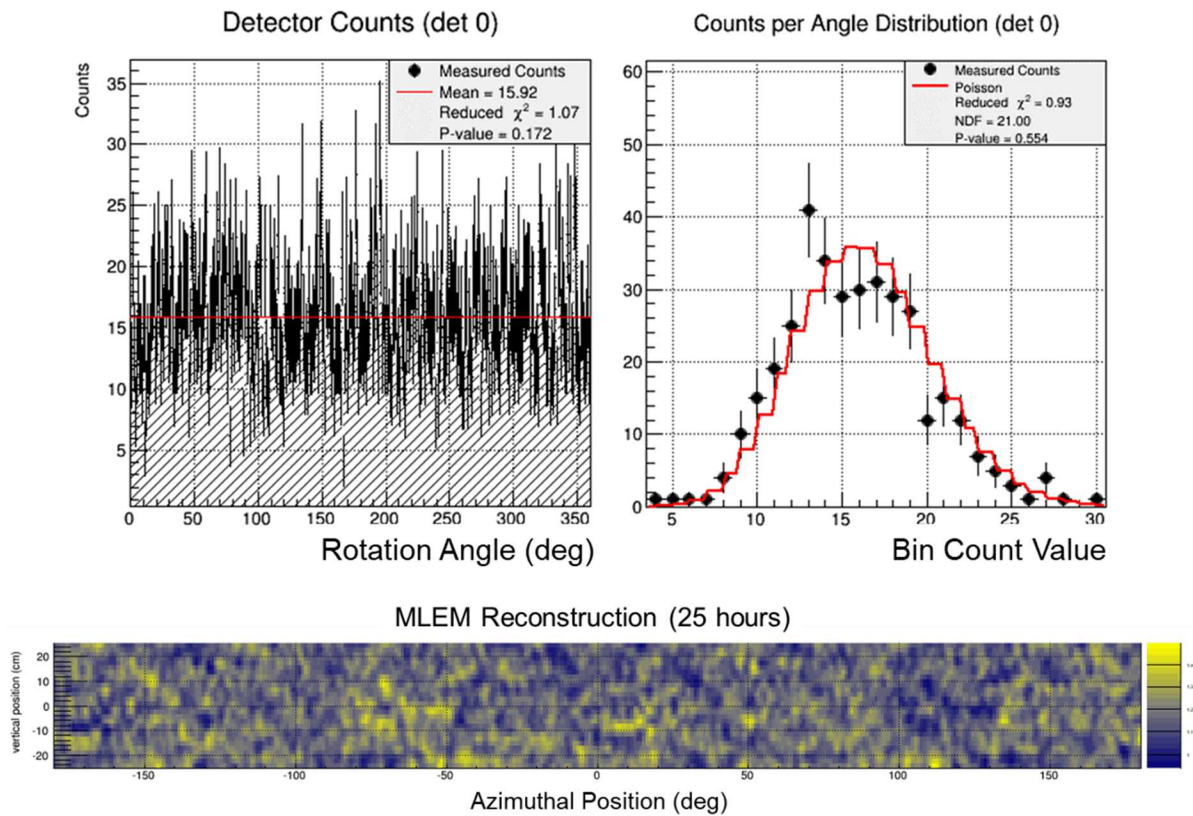


**Figure 5 – The number of fast neutron counts versus mask rotation angle (top left) and distribution of count values per degree (top right) from one detector for a 25-hour measurement of the two matched “true positive” PuO<sub>2</sub> hemispherical shells and the MLEM reconstructed image (bottom).**

In the second experiment, one of the spheres was rotated such that the PuO<sub>2</sub> hemisphere was on the bottom half and the HDPE was on the top half of the sphere. This represents a true negative case in which the two objects are not identical.

. Figure 6 presents the number of counts versus mask rotation angle and distribution of count values in each 1-degree bin. It was found that 15 hours of data was required for statistical convergence. A mean fast neutron count rate of 0.8 neutrons/second provides a mean count value of 15.8 per degree of mask rotation for this dwell time. As was done for the “true positive” case, we test whether the variance of this count distribution is consistent with the expectation of a constant rate by calculating the reduced  $\chi^2$  against the Null hypothesis. Reduced  $\chi^2$  values of 1.34 against the counts vs. rotation angle (Figure 6, top left) and 2.23 against the distribution of count values per degree (Figure 6, top right) are obtained. This corresponds to p-values less than 0.01, indicating that the Null hypothesis is rejected. Therefore, this measurement is *not* statistically consistent with a constant rate indicating failure to confirm that these two items are identical.

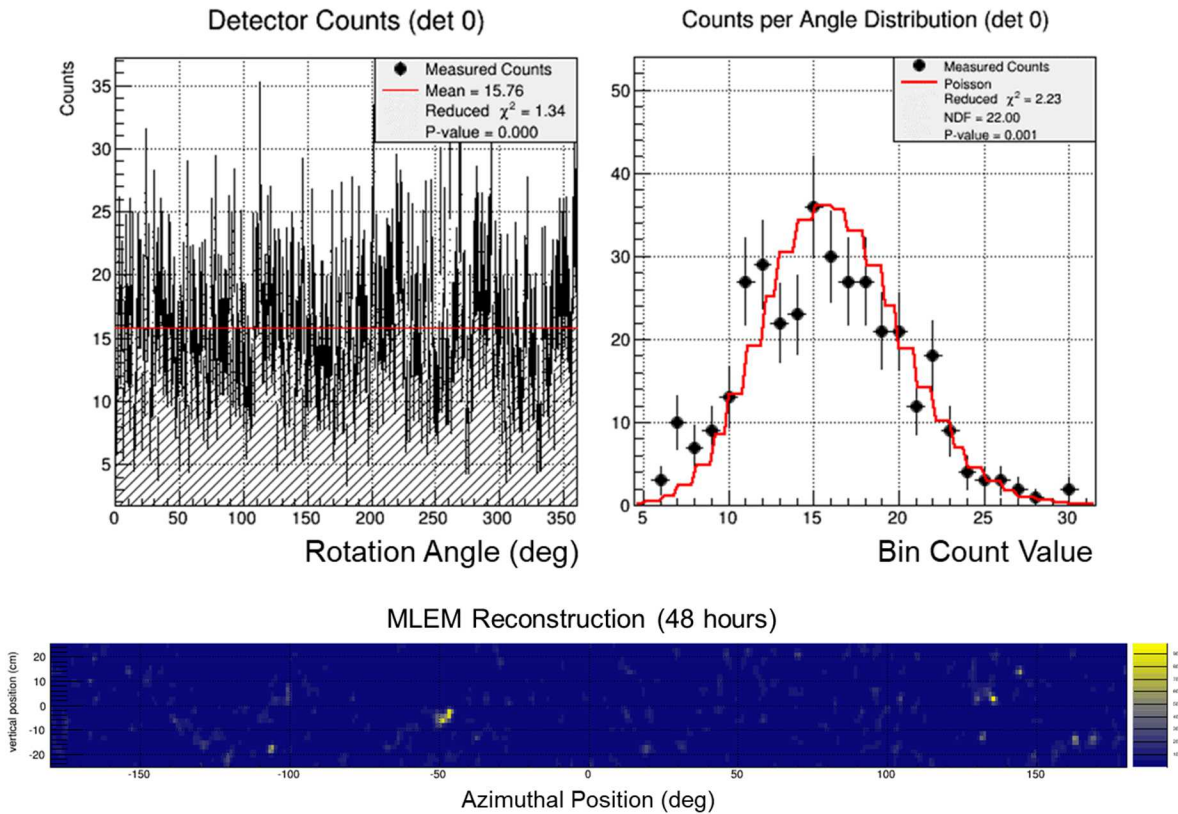


**Figure 6 – The number of fast neutron counts versus mask rotation angle (top left) and distribution of count values per degree (top right) from one detector for a 15 hour measurement of the two PuO<sub>2</sub> hemispherical shells in which one was rotated by 90 degrees, the “true negative” configuration, and the MLEM reconstructed image from a 48 hour measurement (bottom).**

Further, the fast neutron count distribution as a function of mask rotation angle can be used to reconstruct a two-dimensional image MLEM. In this case, the resulting image shown in Figure 6, bottom, does in fact reveal an image exhibiting an excess below a vertical position of zero at about -50 degrees and above zero at about 130 degrees. This is consistent with expectations

given that the horizontal hemispherical shell was at -50 degrees and had excess material on the lower half of the shell when compared with the vertically aligned hemispherical shell. Because there is no neutron emitting material on the upper half of the rotated object, the vertical object at 130 degrees presented excess material on the upper half of the object. That is, the reconstructed image indicates the difference between the two objects being confirmed.

## **Conclusions**

The results presented here demonstrate a promising new method for confirming that two objects have identical volumetric distribution of neutron emitting material while facilitating authentication. In the event of a positive confirmation result, the data is statistically consistent with noise and no sensitive information is recorded. However, an additional layer of information protection can be implemented by not recording the angular orientation of the mask. Because confirmation is indicated by testing whether the data is statistically consistent with a Poisson-distributed random variable, the angular information is unnecessary. It is only required if one wishes to attempt to construct an image. Additionally, since a metric like the reduced  $\chi^2$  metric can be updated in real time, the host and inspector could view the results at intervals during the measurement without risk of revealing potentially sensitive information through a reconstructed image in the event that a negative result is obtained.

Although these experiments were conducted using fast neutron measurements, the CONFIDANTE concept can function with gamma rays or thermal neutrons as well. Using multiple particle types could increase confidence in the verification results because the two objects would also need to have identical gamma and neutron signatures across different energy ranges.

Finally, it should be pointed out that just as is the case with template-based verification methods, at least one measurement must be made with a trusted warhead to gain confidence that all items are not only identical to each other, but also identical to warheads. One advantage of two-item confirmation measurements such as those presented here is that this confidence would then extend to all items that have been or will be confirmed by such measurements. Therefore, it may be reasonable to conduct such measurements with promise that this confidence will be imparted in the future.

## **Acknowledgements**

Sandia National Laboratories is a multimission laboratory managed and operated by National Technology and Engineering Solutions of Sandia LLC, a wholly owned subsidiary of Honeywell International Inc. for the U.S. Department of Energy's National Nuclear Security Administration under contract DE-NA0003525.

## References

1. *Nuclear warhead verification: a review of attribute and template systems.* **J. Yan, A. Glaser.** 157-170, 2015, Science & Global Security, Vol. 23.
2. *Demonstration of Two-dimensional Time-encoded Imaging of Fast Neutrons.* **J. Brennan, E. Brubaker, M. Gerling, P. Marleau, K. McMillan, A. Nowack, N. Renard-Le Galloudec, M. Sweany.** 2015, Nuclear Instruments and Methods A.
3. *An Implementation of Zero Knowledge Confirmation using a Two-dimensional Time-Encoded Imaging System.* **P. Marleau, E. Brubaker.** 2016. INMM Annual Meeting Proceedings.
4. *Maximum Likelihood Reconstruction for Emission Tomography.* **Vardi, L.A. Shepp and Y. 2,** October 1982, IEEE Transactions on Medical Imaging, Vols. MI-1.